Fermi National Accelerator Laboratory

FERMILAB-Pub-95/309-A

Femtolensing and Picolensing by Axion Miniclusters

Edward W. Kolb

Fermi National Accelerator Laboratory
P.O. Box 500, Batavia, Illinois 60510

Igor I. Tkachev

Ohio State University
Columbus, Ohio 43210

September 1995

Operated by Universities Research Association Inc. under Contract No. DE-AC02-76CHO3000 with the United States Department of Energy

Disclaimer

FERMILAB-Pub-95/309-A
OSU-TA-20/95
September, 1995

Femtolensing and Picolensing by Axion Miniclusters

Edward W. Kolb
NASA/Fermilab Astrophysics Group
Fermi National Accelerator Laboratory, Batavia, IL 60510, and
Department of Astronomy and Astrophysics, Enrico Fermi Institute
The University of Chicago, Chicago, IL 60637

Igor I. Tkachev
Department of Physics, The Ohio State University, Columbus, OH 43210, and
Institute for Nuclear Research of the Academy of Sciences of Russia
Moscow 117312, Russia

ABSTRACT

Non-linear effects in the evolution of the axion field in the early Universe may lead to the formation of gravitationally bound clumps of axions, known as "miniclusters." Minicluster masses and radii should be in the range $M_{\rm mc} \sim 10^{-12} M_\odot$ and $R_{\rm mc} \sim 10^{10}$cm, and in plausible early-Universe scenarios a significant fraction of the mass density of the Universe may be in the form of axion miniclusters. If such axion miniclusters exist, they would have the physical properties required to be detected by "femtolensing."

Subject headings: dark matter — axions; gravitational lensing — femtolensing

1. Introduction

Gravitational lensing is now a well established field of astronomy, with a wide variety of astrophysical and cosmological applications. Among the many interesting and important implications of lensing phenomena is the possibility of interference effects between lensed images of point-like astrophysical sources (Mandzhos 1981; Ohanian 1983; Schneider & Schmidt-Burgk 1985; Deguchi & Watson 1986; Peterson & Falk 1991). If the angular separation of the images of a point-like source is comparable to the wavelength of the light, interference between the lensed images will lead to a distinctive fringe pattern both in coordinate space and in energy spectrum. The interference pattern in the energy spectrum will depend upon the location of the detector. Since well separated detectors will see different patterns, there is a distinctive signature of the effect.

If gamma-ray bursters are of cosmological origin they would be small enough to act as point-like sources, and lenses of extremely small masses, $10^{-16}\,M_\odot \lesssim M \lesssim 10^{-13}\,M_\odot$,[1] would produce a frequency-dependent signal in their spectrum (Gould 1992; Stanek et al 1993). For source and lens at cosmological distances, the angular separation of the images would be in the femto-arcsec range, so the phenomenon was dubbed "femtolensing" by Gould (1992).

For source and lens of cosmological distances, the Einstein ring radius is $R_E \sim 3 \times 10^{10}(M/10^{-12}M_\odot)^{1/2}$cm. This means that if two gamma-ray burst detectors are separated by distances larger than R_E, typically one detector will be within the Einstein ring and the other will not. Measurement of different fluxes in two widely separated detectors would extend the detectable range of lens masses to $M < 10^{-7}\,M_\odot$ (Nemiroff & Gould 1995), which can be called picolensing. Thus, femtolensing and picolensing could be a probe of dark matter in a mass range difficult to probe by other means, not to mention settle the issue of the origin of gamma-ray bursters.

Although the phenomenon of femtolensing (henceforth we omit picolensing for brevity, but everywhere below we mean both phenomena) is quite intriguing, the possibility has not attracted a great deal of attention because of a lack of attractive femtolens candidates. Among the front runners in an admittedly weak field are snowballs, black holes, and small molecular clouds. Snowballs (lumps of primordial H and He) are generally believed to evaporate on time scales shorter than the Hubble time (De Rujula et al 1992) and for this reason they are not very attractive. A significant fraction of closure density in black holes in the requisite mass range seems difficult to arrange without a very peculiar spectrum of primordial fluctuations to prevent too many small holes which would be evaporating now. As an unattractive possibility in a field of even more unpalatable choices, small molecular clouds are usually considered the best bet for femtolensing.

---

[1]Post-WKB effects may extend the possible detection range of the lens up to $10^{-11}\,M_\odot$ (Ulmer & Goodman 1995).

Even if one thought of a way to arrange baryons into femto-mass objects, it is unlikely that they would contribute a large enough fraction of closure density for a reasonable optical depth for femtolensing. Even if *all* baryonic matter would form femtolenses, their density is constrained by big-bang nucleosynthesis to be less than about 10% of closure density.

Since non-baryonic dark matter is expected to dominate the mass density of the Universe, perhaps it is easier to arrange a near critical density of *non-baryonic* material into objects capable of femtolensing. But most particle dark matter candidates are very weakly interacting, and they would not be expected to clump on the femtolensing mass and density scales.

In this paper we shall show that the situation may be different if axions are the dark matter. Here we outline a scenario where a significant cosmological density of axion miniclusters (Hogan & Ress 1988; Kolb & Tkachev 1993, 1994a) form with the necessary properties to be natural candidates both for femto- and picolensing.

2. Formation of Axion Miniclusters

The invisible axion is among the best motivated candidates for cosmic dark matter. The axion (Weinberg 1978; Wilczek 1978) is the pseudo-Nambu–Goldstone boson resulting from the spontaneous breaking of a $U(1)$ global symmetry known as the Peccei–Quinn, or PQ, symmetry introduced to explain the apparent smallness of strong CP-violation in QCD (Peccei & Quinn 1977).

There are stringent astrophysical (Dicus et al 1978; Fukugita et al 1982; Hatsuda & Yoshimura 1988; Turner 1988; Raffelt & Seckel 1988; Mayle et al 1988) and cosmological (Preskill et al 1983; Abbott & Sikivie 1983; Dine & Fischler 1983) constraints on the properties of the axion. In particular, the combination of cosmological and astrophysical considerations restrict the axion decay constant f_a and the axion mass m_a to be in the narrow windows $10^{10}\,\mathrm{GeV} \leq f_a \leq 10^{12}\,\mathrm{GeV}$, and $10^{-5}\,\mathrm{eV} \leq m_a \leq 10^{-3}\,\mathrm{eV}$.[2] The contribution to the mean density of the Universe from axions in this window is guaranteed to be cosmologically significant. Thus, if axions exist, they will be dynamically important in the present evolution of the Universe.

The axion is effectively massless well above the QCD confinement temperature of a few hundred MeV. At the confinement scale and below, QCD effects produce a potential for the axion of the form $V(\theta) = m_a^2 f_a^2[1 - \cos(\theta)]$, where the axion field was parametrised as a dimensionless angular variable θ. Above the QCD scale there is no reason for the axion field to be at its low-temperature potential minimum, so as the axion potential turns on the field must relax to the minimum of the potential. Thus

[2]For a review see Turner 1990 or Raffelt 1990.

the energy density in axions corresponds to coherent scalar field oscillations, driven by a displacement of the initial value of the field (the "misalignment" angle) away from the eventual minimum of the temperature-dependent potential.

There will be nothing special in the subsequent evolution of the axion field if the initial misalignment angle is constant throughout the Universe. This may in fact be a reasonable picture if the Universe underwent inflation with the "re-heat" temperature well below f_a. However, equally plausible early-Universe scenarios lead to fluctuations of order unity in the misalignment angle on scales larger than the Hubble radius as the potential starts to develop. Since the final energy density depends upon the initial misalignment angle, spatial fluctuations in the misalignment angle are transformed into spatial fluctuations in the axion density, which later lead to tiny gravitationally bound "miniclusters."

It is easy to understand that miniclusters will be very dense objects. Background axion density scales with temperature as $\bar{\rho}_a(T) = 3T_{\rm eq}s/4$ for $T \ll \Lambda_{\rm QCD}$, where $s \propto T^3$ is the entropy density and $T_{\rm eq}$ is the temperature of equal matter and radiation energy densities. Consider a region with axion over-density, $\rho_a = (1+\Phi)\bar{\rho}_a$, where Φ is larger than unity. The matter density in that region will dominate the radiation density at a temperature $T_\Phi = (1+\Phi)T_{\rm eq}$. At this time the density fluctuation became non-linear, separate out from the cosmological expansion, gravitationally collapse, relax, and form a minicluster with the approximate density it had at T_Φ. A detailed study of this leads to a final minicluster density of (Kolb & Tkachev 1994b)

$$\rho_{\rm mc} \simeq 140\Phi^3(1+\Phi)\bar{\rho}_a(T_{\rm eq}) \approx 3\times 10^{-14}\Phi^3(1+\Phi)\left(\Omega_a h^2\right)^4 {\rm g\ cm^{-3}}. \qquad (1)$$

Even a relatively small increase in Φ is important because the final density depends upon Φ^4 for $\Phi \gtrsim 1$.

In Hogan & Rees (1988) it was assumed that typical values of Φ corresponding to a minicluster are of order unity. The typical mass of a minicluster in Hogan & Rees (1988) was assumed to correspond to the mass of all axions inside the horizon at $T \sim 100$ MeV, with the result $M_{\rm mc} \sim 10^{-5}\,M_\odot$.

In our numerical investigations of the dynamics of the axion field around the QCD epoch (Kolb & Tkachev 1993, 1994a) we found that as the oscillations commence, important, previously neglected, non-linear effects of the field self-interaction can result in the formation of transient soliton-like objects we called axitons. The non-linear effects result in regions with Φ much larger than unity, possibly as large as several hundred, leading to enormous minicluster densities. We also found that the minicluster mass scale is set by the total mass in axions within the Hubble radius at a temperature around $T = T_1 \approx 1$ GeV when axion mass is equal to H. This lowers the minicluster mass from the estimate of Hogan and Rees to about $10^{-12}M_\odot$.

Our previous calculations suggested that miniclusters could be a candidate for femtolensing. We have since extended and improved our original calculation of the properties of axion miniclusters using the same approach as in Kolb & Tkachev 1993, but with better numerical resolution and

using a different spectrum of initial fluctuations of θ. The new calculation confirmed the basic picture of minicluster formation and sharpened the predictions of the masses, radii, and abundance of miniclusters. In the next section we summarize the results relevant for femtolensing.

3. Physical Properties of Axion Miniclusters

The evolution of the axion field in an expanding, spatially flat Universe during the epoch when axion mass switches on is governed by a wave-like equation with a non-linear, time-dependent potential (Kolb & Tkachev 1993):

$$\psi'' - \Delta^2\psi + \eta^{n+3}\sin(\psi/\eta) = 0 \ , \tag{2}$$

where $\psi \equiv \eta\theta$, $\psi'' \equiv d^2\psi/d\eta^2$, η is the conformal time (normalized to $\eta = 1$ when the inverse of the axion mass is equal to the Hubble radius—i.e., $\eta(T_1) \equiv 1$), and Δ is the Laplacian with respect to comoving coordinates. The factor of n in this equation arises from the way the potential develops due to instanton effects: $m_a^2(\eta) = m_a^2(\eta = 1)\eta^n$, with $n = 7.4 \pm 0.2$ (Gross et al 1981).

As an initial conditions in the new calculation we considered the possibility that the main source of axions is provided by the decay of axion strings prior to $T = T_1$ (Davis 1986; Harari & Sikivi 1987; Battye & Shellard 1994). This might be expected if the reheating temperature after inflation is larger than the temperature of the Peccei-Quinn phase transition. In such a scenario the spectral energy density of axions produced by string decay corresponds to a power law: $d\rho_a/d\omega \propto \omega^{-1}$, where $\omega = |k|$ (recall that the axion effectively is massless prior to $\eta = 1$). This corresponds to $|a(k)| = \text{const} \times k^{-5/2}$ for the Fourier amplitudes of the axion field. In our latest calculations we used initial conditions at $\eta = 1$ with amplitudes of the Fourier modes corresponding to the above spectrum and with random phases. Overall amplitude was chosen to ensure rms value of θ to be $\pi/\sqrt{3}$.

The final density distribution of axions in one of the 2-dimensional slices through the integration volume is shown in Figure 1. Three high amplide density peaks which are seen on this figure results from non-linear interaction and are absent in the case of the harmonic potential. They form miniclusters of interest at $T \sim \Phi T_{\rm eq}$. The evolution of the axion field with the above initial conditions was qualitatively similar to the evolution using the white-noise initial conditions of our previous calculations. From the results of the numerical calculation we determined the mass, radius, and abundance of axion miniclusters.

3.1. Minicluster mass. The mass of axion minicluster is set by the scale when axion oscillations commence. As mentioned above, we have defined T_1 as a temperature when the axion mass equals the Hubble constant, $m_a(T_1) = H(T_1)$. Using results of Turner (1986) we use $T_1 = (f_a/10^{12}\text{GeV})^{-0.175}\,(\Lambda_{\rm QCD}/200\text{MeV})^{0.7}$ GeV. In what follows we assume $T_1 = 1$ GeV. As a

reference mass scale we define the mass of all axions in a cubic volume of length equal to the Hubble length at T_1, and density equal to the mean cosmological density: $M_1 = \pi^2 g_*(T_1) T_1^3 T_{\rm eq}/30 H_1^3$, where $g_*(T_1) \approx 62$ is the number of an effectively massless degrees of freedom at temperature T_1. Using $H = 1.66 g_*^{1/2} T^2/M_{\rm Pl}$ we find $M_1 = 8.2 \times 10^{-12} \Omega_a h^2\, M_\odot$.

Our numerical integration of equation (2) shows that there is a spectrum of minicluster masses, but typically the mass of the axion minicluster is a reasonable fraction of M_1, $M_{\rm mc} \lesssim 0.1 M_\odot$. We estimate the average minicluster mass to be of order $M_{\rm mc} \sim 10^{-12}\, M_\odot$.

Masses of miniclusters are relatively insensitive to the particular value of Φ associated with the minicluster.

3.2. Minicluster radius. Typical axion miniclusters have a large density contrast, $\Phi \gtrsim 1$ (Kolb & Tkachev 1993), see Figure 1. Equation (1) gives the minicluster radius as a function of M and Φ:

$$R_{\rm mc} \approx 2 \times 10^{11} \Phi^{-1} \left(1+\Phi\right)^{-1/3} \left(\Omega_a h^2\right)^{-1} \left(\frac{M}{10^{-12} M_\odot}\right)^{1/3} {\rm cm}\,. \tag{3}$$

The radius of a particular minicluster depends upon its associated value of Φ. In the limit $\Phi \gtrsim 1$ the radius of a minicluster scales as $\Phi^{-4/3}$.

3.3. Minicluster abundance. From the numerical calculation we have extracted the mass fraction of axions in density peaks of Φ larger than a given value Φ_0. It is plotted for several values of conformal time $\eta = 1, 3$, and 4 in Figure 2. By the time $\eta > 4$ we are no longer able reliably to resolve the highest density peaks because density contrasts became too large for our 256^3 grid. Although at $\eta = 4$ the evolution has not completely frozen out, (especially at the large-Φ end) we can set a lower bound for the density fractions, e.g., more than 13% are in miniclusters with $\Phi > 10$ and 70% of all axionic dark matter are in miniclusters ($\Phi > 1$), see Figure 2.

4. Miniclusters as Femtolens

For axion miniclusters (or, for that matter, any other possible candidate) to be detected by femtolensing (or picolensing) the following three conditions must be satisfied:

i.) The minicluster has to be in the mass range, $10^{-16}\, M_\odot \lesssim M_{\rm mc} \lesssim 10^{-11}\, M_\odot$ (Gould 1992; Ulmer & Goodman 1995) for femtolensing, or $M_{\rm mc} \lesssim 10^{-7}\, M_\odot$ (Nemiroff & Gould 1995) for picolensing.

ii.) The physical radius of the minicluster has to be smaller than its Einstein ring radius. For source and lens of cosmological distance the Einstein ring radius is, see e.g. Press & Gunn (1973):

$$R_{\rm E} \lesssim 3 \times 10^{10} h^{-1/2} \left(\frac{M}{10^{-12} M_\odot}\right)^{1/2} {\rm cm}, \tag{4}$$

where as usual $H_0 = 100h$ km s^{-1}Mpc^{-1}.

iii.) The third condition is that a significant fraction of the total mass density of the Universe must be in the form of miniclusters, say $\Omega_{\rm mc} \sim 0.1$, for the lensing rate to be reasonable. This condition is independent upon the lens mass (Press & Gunn 1973).

These conditions are non-trivial, which is why there were no serious candidates for femtolensing. But we shall now demonstrate that all three conditions are naturally met for the case of axion miniclusters.

That miniclusters satisfy the mass condition follows from the fact that the minicluster mass is determined by the total mass of axions within the Hubble radius at $T \sim 1$ GeV. Of course there will be some spread in minicluster masses, but as discussed in the previous section, the masses should be peaked around $10^{-12}M_\odot$, well within the desired range for lensing.

Using the radius of miniclusters from equation (3) and the Einstein ring radius from equation (4), we find $R_E/R_{\rm mc} \simeq 0.15\Phi\,(1+\Phi)^{1/3}\,\Omega_a h^{3/2}\,(M/10^{-12}M_\odot)^{1/6}$. The requirement that miniclusters be smaller than their Einstein ring radius places restrictions on Φ as a function of M. We see that if $\Omega_a \sim 1$, then miniclusters with $M \sim 10^{-12}M_\odot$ and $\Phi \gtrsim 5 - 10$ (depending upon h) are within their Einstein ring radius. Actually, objects with the radius comparable to their Einstein radius have a better chance to be detected as femtolenses (compared to point mass objects) if they are in the mass range $10^{-11}M_\odot \lesssim M \lesssim 10^{-13}M_\odot$ (Ulmer & Goodman 1995). From Figure 2 we see that more than about 20% of all dark matter axions are in miniclusters with $\Phi \gtrsim 5$ and will be within their ring radius.

We conclude that if axions are the dark matter with Ω_a close to unity, then the fraction of Ω in miniclusters capable of femtolensing is 15% - 20% (see Fig. 2), i. e. will be in excess of 10%—large enough to result in a detectable rate.

Since miniclusters in the IGM as well as in galactic halos contribute to femtolensing events, questions such as: how are they clustered, do miniclusters survive the epoch of galaxy formation, are they disrupted in their encounters with stars, etc., may be irrelevant here. Since large-Φ miniclusters are very dense, form early, and are well separated from each other, they should escape mutual disruption and merging.

It can be important for the present discussion that miniclusters with $\Phi \gtrsim 30$ relax to Bose-stars (Tkachev 1991; Kolb & Tkachev 1993) and consequently became even densier and compact.

We conclude that axion miniclusters are candidates for femtolensing and picolensing. We do not believe that the conclusion is sensitive to specific initial conditions, but is generic so long as there are large super-horizon-sized fluctuations in the misalignment angle during the development of the axion potential.

We thank S. Colombi, A. Gould and A. Stebbins for useful discussions. This work was supported by DOE and NASA grant NAG 5-2788 at Fermilab and DOE grant DE-AC02-76ER01545 at Ohio.

REFERENCES

Abbott, L. F., & Sikivie, P. 1983, Phys. Lett., 120B, 133

Battye, R. A., & Shellard, E. P. S. 1994, Phys. Rev. Lett., 73, 2954

Davis, R. 1986, Phys. Lett., 180B, 225

Deguchi, S., & Watson, W. D. 1986, ApJ, 307, 30

De Rujula, A., Jetzer, P., & Massó , E. 1992, A&A, 254, 99

Dicus, D. A., Kolb, E. W., Teplitz, V. L., & Wagoner, R. V. 1978, Phys. Rev. D, 18, 1829

Dine M., & Fischler, W. 1983, Phys. Lett., 120B, 137

Fukugita, M., Watamura, S., & Yoshimura, M. 1982a, Phys. Rev. Lett., 48, 1522

Gould, A. 1992, ApJ, 386, L5

Gross, D., Pisarski, R., and Yaffe, L. 1981, Rev. Mod. Phys., 53, 43

Harari D., & Sikivie, P. 1987, Phys. Lett., 195, 361

Hatsuda, T., & and Yoshimura, M. 1988, Phys. Lett., 203B, 469

Hogan, C. J., & Rees, M. J. 1988, Phys. Lett., 205B, 228

Kolb, E. W., & Tkachev, I. I. 1993, Phys. Rev. Lett., 71, 3051

Kolb, E. W., & Tkachev, I. I. 1994a, Phys. Rev. D, 49, 5040

Kolb, E. W., & Tkachev, I. I. 1994b, Phys. Rev. D, 50, 769

Mandzhos, A. V. 1981, Soviet Astron. Lett., 7, 213

Mayle, R., Wilson, J. R., Ellis, J., Olive, K. A., Schramm, D. N., & Steigman, G. 1988 Phys. Lett., 203B, 188

Nemiroff, R. J., & Gould, A. 1995 Ohio State University Preprint OSU-TA-9/95, ApJletters in press.

Ohanian, H. C. 1983, ApJ, 271, 551 (1983)

Peccei, R. D., & Quinn, H. 1977 Phys. Rev. Lett., 38, 1440

Peterson, J. B., & Falk, T. 1991, ApJ, 374, L5

Preskill, J., Wise M., & Wilczek, F 1983, Phys. Lett., 120B, 127

Press, W. H. & Gunn, J. I. 1973, ApJ, 185, 397

Raffelt, G. G., & and Seckel, D. 1988, Phys. Rev. Lett., 60, 1793 (1988)

Raffelt, G. G. 1990, Phys. Rep., C198, 1

Schneider, P., & Schmidt-Burgk, J. 1985, A&A, 148, 369

Stanek, K. Z., Paczynski, B., & Goodman, J. 1993, ApJ, 413, L7

Tkachev, I. I. 1991, Phys. Lett., B261, 289

Turner, M. S. 1986, Phys. Rev. D, 33, 889

Turner, M. S. 1988, Phys. Rev. Lett., 60, 1797

Turner, M. S. 1990, Phys. Rep., C197, 67

Ulmer, A., & Goodman, J. 1995 ApJ, 442, 67

Weinberg, S. 1978, Phys. Rev. Lett., 40, 223

Wilczek, F. 1978, Phys. Rev. Lett., 40, 279

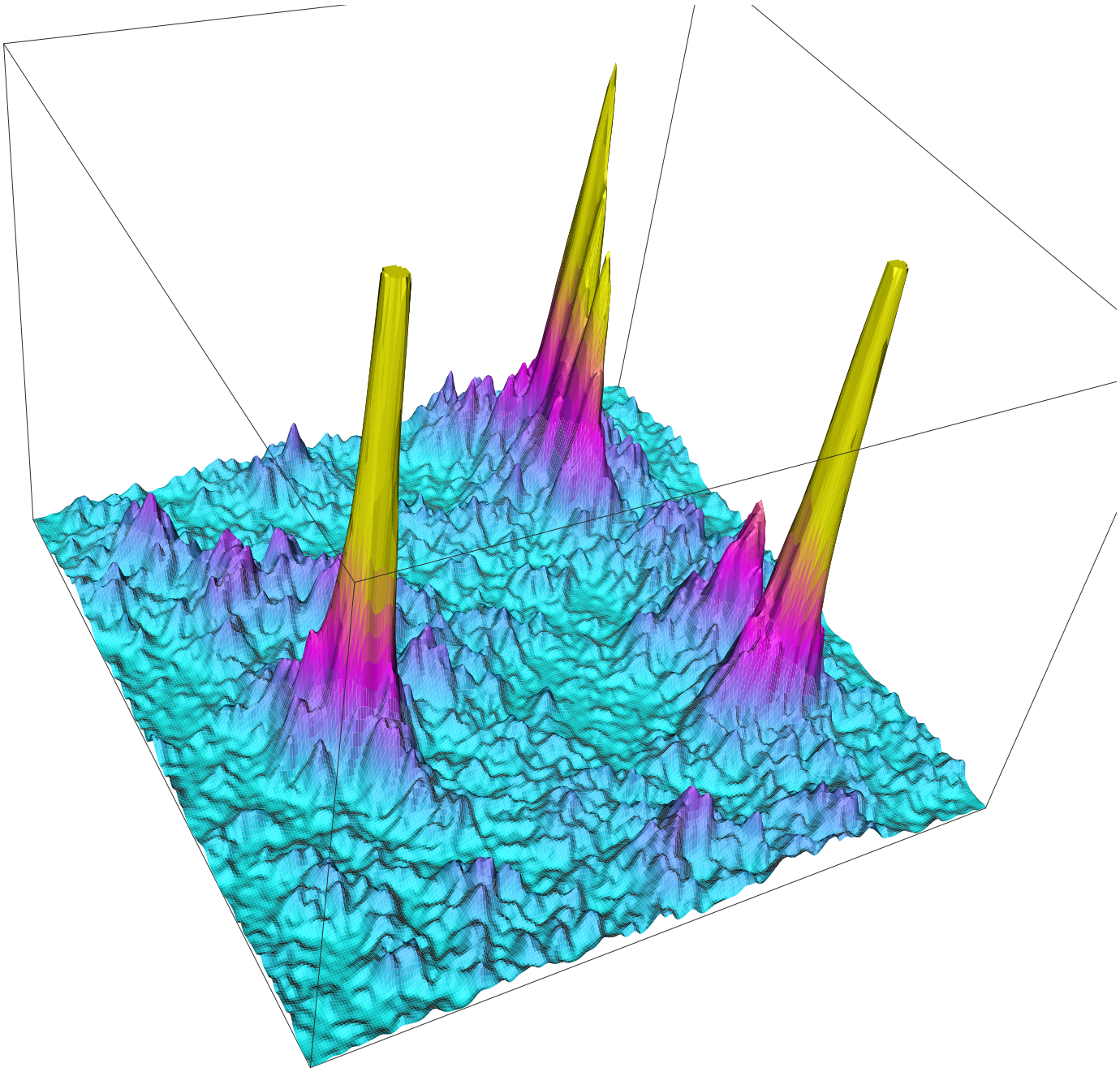

Fig. 1.— This is a two-dimensional slice through a three dimensional box showing the distribution of axion energy densities for $T \gg T_{\rm eq}$. The height of the plot corresponds to $\Phi = \delta\rho_a/\bar{\rho}_a = 20$, and the width to a length of $4H^{-1}(T_1)$ (this corresponds to a comoving length of about 0.2 pc).

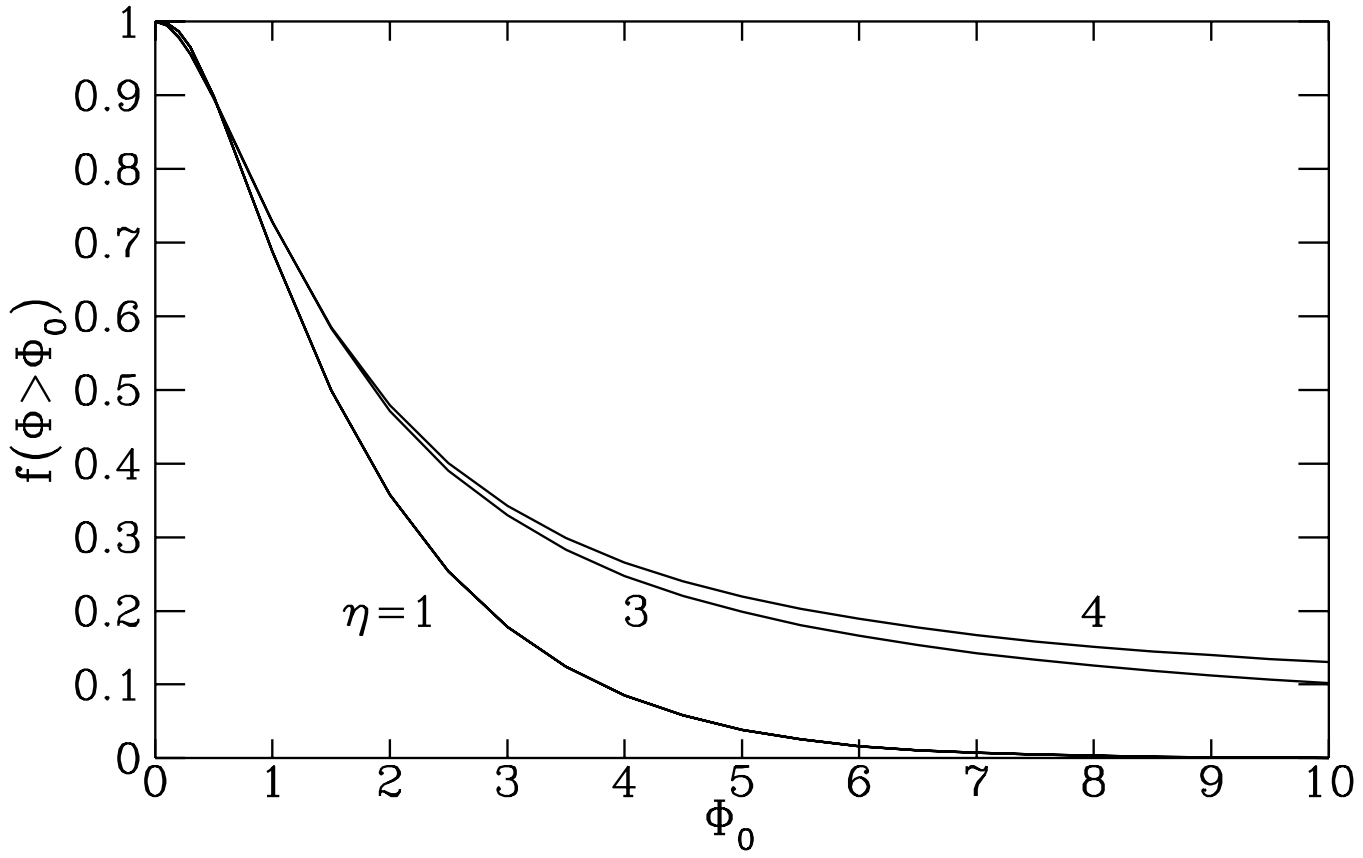

Fig. 2.— The mass fraction of axions in miniclusters with Φ greater than Φ_0 as a function of Φ_0. By $\eta = 4$ the evolution has very nearly frozen.